SOUTHAMPTON OCEANOGRAPHY CENTRE

RESEARCH & CONSULTANCY REPORT No. 88

The impact of aerosol loading on estimates of the surface shortwave flux in the SOC climatology

J P Grist and S A Josey

2004

COAPEC Project - Balancing the Atlantic Heat and Freshwater Budgets, Report No. 2

James Rennell Division for Ocean Circulation and Climate
Southampton Oceanography Centre
University of Southampton
Waterfront Campus
European Way
Southampton
Hants SO14 3ZH UK
Tel: +44 (0)23 8059 7738
Fax: +44 (0)23 8059 6400
Email: jyg@soc.soton.ac.uk

DOCUMENT DATA SHEET

AUTHOR
GRIST, J P & JOSEY, S A

PUBLICATION DATE
2004

TITLE
The impact of aerosol loading on estimates of the surface shortwave flux in the SOC climatology. (COAPEC Project - Balancing the Atlantic Heat and Freshwater Budgets, Report No. 2)

REFERENCE
Southampton Oceanography Centre Research and Consultancy Report, No. 88, 15pp. & figs. (Unpublished manuscript)

ABSTRACT

The uncertainty in empirical estimates of the shortwave flux in the Southampton Oceanography Centre (SOC) air-sea flux climatology due to neglect of tropospheric aerosols is investigated. The SOC shortwave flux fields were derived using a formula originally developed from data in an area of low aerosol loading and do not take into account the variability of aerosol content over the global ocean. We use the method of Tragou et al. (1999) to estimate the reduction that should be applied in order to correct for the effects of aerosol loading. Our results suggest that the mean global effect of not specifying atmospheric aerosol content is that the SOC shortwave flux is an overestimate, but by no more than 2 Wm^{-2}. This equates to less than 7% of the global bias in the original climatology. At a regional level, the effect of the aerosols may be up to 40 Wm^{-2} in the tropical Atlantic and the Arabian Sea. Independent measurements of the shortwave flux from research buoys and satellites provide some support for our results. However, further analyses are required as only a few independent buoy measurements are currently available in regions of high aerosol loading.

KEYWORDS

aerosols, air-sea fluxes, Arabian Sea,, COAPEC, project, shortwave radiation, SOC climatology

ISSUING ORGANISATION

Southampton Oceanography Centre
University of Southampton
Waterfront Campus
European Way
Southampton SO14 3ZH
UK

ABSTRACT

The uncertainty in empirical estimates of the shortwave flux in the Southampton Oceanography Centre (SOC) air-sea flux climatology due to neglect of tropospheric aerosols is investigated. The SOC shortwave flux fields were derived using a formula originally developed from data in an area of low aerosol loading and do not take into account the variability of aerosol content over the global ocean. We use the method of Tragou et al. (1999) to estimate the reduction that should be applied in order to correct for the effects of aerosol loading. Our results suggest that the mean global effect of not specifying atmospheric aerosol content is that the SOC shortwave flux is an overestimate, but by no more than 2 Wm^{-2}. This equates to less than 7% of the global bias in the original climatology. At a regional level, the effect of the aerosols may be up to 40 Wm^{-2} in the tropical Atlantic and the Arabian Sea. Independent measurements of the shortwave flux from research buoys and satellites provide some support for our results. However, further analyses are required as only a few independent buoy measurements are currently available in regions of high aerosol loading.

1. INTRODUCTION

This report forms part of a series describing results from a Natural Environment Research Council (NERC) Coupled Ocean-Atmosphere Processes and European Climate (COAPEC) funded project, which has the primary aim of producing a balanced set of ocean-atmosphere heat exchange fields using the existing Southampton Oceanography Centre (SOC) climatology as a basis. It is well recognised that ship-based estimates of air-sea heat fluxes, have thus far been unable to produce a balanced ocean heat budget. In particular, the SOC climatology has a global mean oceanic heat gain of approximately 30 Wm^{-2}. Attempts to correct for this bias to date have taken the form of identifying and correcting for errors in ship observations (Kent et al., 1993), developing new flux formulae (Josey et al., 2003) and adjusting the component fluxes with inverse analysis techniques (Grist and Josey, 2003, 2004). In this report we investigate if part of the ocean heat gain in the SOC climatology is due to a bias in the empirical shortwave formula.

In the SOC climatology the clear sky shortwave radiation is estimated from the empirical formula of Reed (1977). The Reed formula does not include a dependency on the atmospheric aerosol content and was derived using data from 3 mid-latitude sites where the aerosol loading was relatively low. Aerosols absorb and reflect incoming solar radiation and thereby act to reduce the surface shortwave flux. It has thus been suggested that the Reed formula may overestimate the shortwave flux in regions of high aerosol loading (Gilman and Garrett, 1994). Indeed, this overestimate of the shortwave flux (which hereafter we refer to as the aerosol effect) has been observed in the Red Sea (Tragou et al., 1999) and the Mediterranean Sea (Tragou and Lascaratos, 2003). Tragou et al. (1999) developed a method for correcting for this bias using satellite-derived estimates of Aerosol Optical Thickness (SAOT). In this study we utilize their method, which we refer to as the Tragou method, to estimate the importance of the aerosol effect over the global ocean. In doing this we will explore the question of how significant the aerosol effect is in terms of the SOC climatology's 30 Wm^{-2} bias.

The structure of the report is as follows. In Section 2, the data used in the study is described. In Section 3, we discuss the parameterisation of the shortwave flux formula and the method for adjusting the shortwave flux. The results of applying the adjustment are described in Section 4. Finally, we summarise and discuss the implications of the results in Section 5.

2. DATA

2.1 The SOC Climatology

The primary data set for our study is the SOC climatology which has been extensively described elsewhere (Josey et al., 1998; 1999). It was derived from voluntary observing ship reports in the Comprehensive Ocean - Atmosphere Dataset 1a (Woodruff et al., 1993), covering

the period 1980-1993. Additional information regarding observing procedure was merged onto this dataset from the International List of Selected, Supplementary and Auxiliary Ships, which is published annually by the World Meteorological Organisation (e.g. WMO 1993). The method used for the production of the climatology is fully described in Josey et al. (1998). Results from an evaluation of the climatology using hydrographic and research buoy measurements are discussed in Josey et al. (1999). In this report, we examine the SOC climatological mean fields of the shortwave flux that were determined using the shortwave flux formula described later in Section 3.

2.2 Satellite Aerosol Optical Thickness (SAOT)

Following Tragou et al. (1999), the distribution of atmospheric aerosol is determined using a dataset of monthly mean values of SAOT from the period July 1989 - June 1991. SAOT is a National Oceanographic and Atmospheric Administration (NOAA) product with a 1° by 1° global coverage (Stowe et al., 1997; Husar et al., 1997). This dataset was derived using observations of backscattered solar radiation from the polar orbiting Advanced Very High Resolution Radiometer (AVHRR) satellite. It is possible to calculate the SAOT because aerosols backscatter solar radiation in proportion to the aerosol optical thickness. The optical thickness is by definition related to the transmittance and thus can potentially provide a correction for the shortwave flux. Unfortunately, the AVHRR SAOT cannot be simply related to the transmission coefficient of clear sky radiation. This is because it does not provide the required information about aerosol size, shape and composition (Lacis and Mishchenko 1995). However, Tragou et al. (1999) have described a method, whereby with some ground truth calibration, the SAOT can be used to produce a correction due to aerosol scattering. This method, which is utilised in this study, is described more fully in Section 3.

2.3 Other Independent Data Sources

To evaluate the estimates of the aerosol effect that we derive using the SAOT dataset and Tragou's method, various independent data sources were utilised. In particular, we have used surface measurements of shortwave radiation made on 5 Woods Hole Oceanographic Institution (WHOI) research buoy deployments (e.g. Moyer and Weller, 1997) during the period of the SOC climatology. Details of the buoy deployments are given in Table 1; note these buoys have been previously used for other evaluations of the SOC fluxes (Josey et al., 1999; Grist and Josey, 2003).

Estimates of surface shortwave over the global ocean were also provided from the Quality-Check Shortwave (QCSW) algorithm of the Global Energy and Water Cycle Experiment / Surface Radiation Budget Experiment (GEWEX/SRB) project Release 2 (known as The Langley Parameterised Shortwave Algorithm (LPSA), Gupta et al., 2001). The LPSA shortwave flux is derived from a radiative transfer model in which the required inputs of cloud parameters, column precipitable water and column ozone were taken from the International Satellite Cloud Climatology Project (ISCCP) – C1 data sets (Rossow and Schiffer 1991). The values of surface albedo were taken from formulae in the literature and the values of the top of the atmosphere

albedo were taken from the results of the Earth Radiation Budget Experiment (ERBE) (Barkstrom et al., 1989). One limitation of the LPSA dataset is that there is very little spatial variability prescribed in the aerosol properties. Essentially there is one aerosol type for maritime regions and one for coastal regions and a dependency on the solar zenith angle.

Shortwave flux estimates over the global ocean were also taken from the ISCCP FD data product (Zhang et al., 2003). These estimates were obtained using the NASA Goddard Institute for Space Studies (GISS) climate GCM radiative transfer algorithm. The required input to the algorithm includes cloud and surface properties every 3 hours from ISCCP, daily atmospheric profiles of temperature and humidity from the NOAA TIROS Operational Vertical Sounder (TOVS), daily ozone abundances from the Total Ozone Mapping Spectrometer (TOMS), and a climatology of cloud vertical layer distributions from rawinsonde humidity profiles (Wang et al., 2000). In contrast to the LPSA product, the FD product is derived using information on the spatial distribution of tropospheric aerosols in the form of a climatology from the NASA GISS climate model.

3. METHOD

3.1. The Shortwave Parameterisation

In the SOC climatology (Josey et al., 1998) and in Tragou et al. (1999) the monthly mean net shortwave flux is derived from the following formula:

$$Q_s = Q_{cs}(1 - 0.62n + 0.0019h)(1-\alpha) \quad (1)$$

where n is the cloud fraction; h is the solar altitude in degrees; α is the albedo of the sea surface from Payne (1972). Q_{cs} is the clear sky irradiance. Equation 1 represents the cloud reduction formula of Reed (1977) together with a parameterisation for the clear sky irradiance Q_{cs}. The Reed formula has no dependence on the spatial variability of tropospheric aerosols as it was derived in a region of low aerosol loading. Consequently, it may be expected to overestimate the shortwave flux in regions of high aerosol loading. This has been found to be the case for the Mediterranean and Red Seas (Tragou et al., 1999; Tragou and Lascaratos, 2003). The Tragou method for making an adjustment to the shortwave estimate based on the SAOT variability is described below.

Before considering the method in detail, we first note that the clear sky irradiance is dependent on solar geometry and has been calculated using a number of variants on the same basic formula. Tragou et al. (1999) use the formulation of Rosati and Miyakoda (1988):

$$Q_{cs} = 1/2[T^{1/\cos z} + (1 - A)]\ Q_0 = Q_0 f \quad (2)$$

where T = 0.7 is the transmission factor for a clear atmosphere; z is the solar zenith angle; A = 0.09 is the absorption factor; $Q_0 = S_0 \cos z$, where the solar constant $S_0 = 1370\ Wm^{-2}$, and $f = 1/2 [T^{1/\cos z} + (1 - A)]$. The SOC climatology uses a variant of this formula due to Seckel and Beaudry (1973), details of which are given in Reed (1977).

3.2 The Tragou Method

Tragou et al. (1999) described a method for adjusting the calculated insolation Q_s at the sea surface to account for the influence of aerosols. The method was initially used in the Red Sea. The goal of the Tragou method is to determine a transmission coefficient anomaly Tr*(x, y, t) which adjusts the shortwave based on the spatial and seasonal distribution of SAOT. Having determined this, a revised shortwave estimate can be made:

$$Q_s' = Q_s Tr^* \quad (3)$$

The steps for calculating the transmission coefficient anomaly are as follows. First define a transmission coefficient anomaly $Tr_m^*(t)$, which varies only with the month of the year, as the ratio of the irradiance observed by ground truth solarimeters (Q_{sg}) to the estimated shortwave flux Q_s (Equation 1):

$$Tr_m^* = Q_{sg}/Q_s \qquad t = 1, 2,...12 \quad (4)$$

Here, errors in the ground based measurements are taken to be much smaller than those due to the aerosol effect so that the ground values can be assumed to accurately measure the true net shortwave. Tragou et al. (1999) calculated $Tr_m^*(t)$ at 3 World Radiation Data Centre Red Sea coastal stations and subsequently used the smoothed mean of the values obtained, which were broadly similar in each case. Rewriting (4) for clear sky conditions we have:

$$Q_{sgc}(t) = Q_0 f\ Tr_m^* \quad (5)$$

where Q_{sgc} is the ground-based observation of clear sky irradiance.

Now the AVHRR satellite data (Husar et al., 1997) gives the spatial (x, y) and temporal (t) variability of the aerosol optical thickness index (τ^A_s) or SAOT from which a transmission coefficient due to aerosol scattering may be calculated:

$$Tr^A_s = \exp(-\tau^A_s/\cos z) \qquad (6)$$

In the Tragou method, the clear sky insolation at the sea surface is then written as:

$$Q_{csA} = Q_0 f_c Tr^A_S \quad (7)$$

where the coefficient f_c is the constant of proportionality for the attenuation of Q_0 due to absorption and scattering by atmospheric molecules and absorption by aerosols, as measured by Tr^A_s. By requiring that the clear sky insolation estimate from (7) be equal to the measured clear sky insolation (5) it is then possible to determine f_c:

$$f_c = f\ (Tr_m^*/Tr^A_s) \qquad (8)$$

Tragou et al. (1999) then produced twelve monthly values of f_c by using the smoothed monthly values of Tr_m^*, monthly means of Tr^A_s (from the grid point nearest the ground truth station) and monthly values of the parameter f, which was defined in (2).

Having calibrated f_c in this way using the coastal stations, Tragou et al. (1999) were then able to calculate spatially and seasonally varying values of Tr*(x, y, t) for the Red Sea as a whole using,

$$Tr^*(x, y, t) = [f_c(t)/f(t)]\ Tr^A_s(x, y, t) \qquad (9)$$

Finally, they were then able to produce corrected estimates of the shortwave flux by multiplying the original flux by Tr*(x, y, t) according to (3).

For our study, we have extended the Tragou method to the global ocean using an annual mean value for f_c of 0.9 determined from their analysis. We have also limited the value of Tr* (x, y, t) to be less than 1 as unrealistically large values can otherwise occur at high latitudes where Tr^{A}_{s} is small due to low aerosol loading. This probably indicates that their technique requires further calibration before it can be used in these regions. Nevertheless we expect our results to provide a reasonable estimate of the effects of neglecting aerosols in regions of high loading at lower latitudes.

4. RESULTS

4.1 Shortwave and SAOT Fields

The SOC shortwave fields for the months of January, April, July and October (hereafter JAJO) are shown in Fig. 1. As described elsewhere (Josey et al., 1998) the seasonal march is determined primarily by variations in the solar elevation. The zonal band of maximum radiation migrates between about 23° N and 23° S. The azonal variation in the shortwave flux is determined by the variation in cloud cover. The position of the Inter-Tropical Convergence Zone is evident in the zonal mean variation as a local minimum just north of the equator.

The monthly mean fields of SAOT for JAJO are shown in Fig. 2. Some confidence in the AVHRR product is gained from the fact that high values are consistent with known sources of atmospheric aerosols and the relevant meteorology. An area of high aerosol loading off the east coast of Asia is evident in all months. This is probably associated with industrial pollutants from the east coast cities. In April this feature is a particularly well-developed plume stretching northeast across the Pacific. A similar plume is seen stretching northeast across the Atlantic from the urban areas on the east coast of the USA in July. The dust plume associated with westward blown Saharan dust is evident throughout the year in the tropical North Atlantic. In addition, in July and October, a plume associated with southern African biomass burning is evident in the southern Atlantic. Finally in July, the Arabian Sea experiences very high aerosol loading. This is associated with monsoonal winds transporting dust from the surrounding desert regions (Husar et al., 1997).

It is important to highlight three areas in which there is some ambiguity in interpreting the aerosol fields. Firstly, at 50° S there is a band of relatively high SAOT values in January. It has been suggested that this is associated with strong emission of oceanic sulphur aerosols. However this is inconsistent with modelling studies of the global sulphur cycle which place this band a further 10° to the south (Chin et al., 1996). Secondly, there is some question over the source of the large plume located over the equatorial North Pacific in April. Husar et al (1997) note that the evidence does not suggest that the source of this plume is oceanic. It has been suggested that the source of the plume is central American pollution. However this idea is also questionable given the large area the plume covers. Thirdly, a comparison with the TOMS Aerosol Index indicates that the AVHRR product does not clearly illustrate the plume in the tropical South Atlantic associated with South American biomass burning. It has been suggested that this weak detection,

particularly in July and October, is in part due to the extensive cloud cover at the same time (Husar et al., 1997).

4.2 Adjustments for the Aerosol Effect

The spatially and seasonally varying transmission coefficient anomaly Tr*(x, y, t), for JAJO is shown in Fig. 3. The areas where values of Tr*(x, y, t) are significantly < 1 correspond primarily to the regions of high SAOT noted above. The greatest reductions occur in the tropical Atlantic in all months of the year and the Arabian Sea in July where the minimum value for Tr*(x, y, t) approaches 0.5. Note that there are some areas, particularly in the high latitudes of the winter hemisphere where Tr*(x, y, t) is greater than 1. As noted in Section 3, values of Tr*(x, y, t) > 1 are set equal to 1 for subsequent calculations of the shortwave adjustment because of the uncertainty in the validity of the Tragou method under conditions of low aerosol loading.

Annual means of the adjustment to the shortwave flux calculated by the Tragou method, the original SOC shortwave flux and the adjusted flux are shown in Fig. 4. The largest adjustments, up to 50 Wm^{-2}, are made in the eastern tropical Atlantic. The feature resembling the Saharan dust plume stretches westward, as its magnitude diminishes. In the Caribbean, adjustments of the order 15 Wm^{-2} are required. There is still evidence of the Saharan plume to the west of South America in the tropical Pacific. In those areas the adjustments are generally less than 10 Wm^{-2} although some of the aerosols may be associated with industrial or urban pollution from Central America. Another region with large adjustments is the area encompassing the Red Sea, the Gulf of Arabia and the Arabian Sea where the adjustments are of the order 40 Wm^{-2}. By comparison the adjustments made in the Mediterranean are somewhat smaller, between 10 and 15 Wm^{-2}. Adjustments of just over 20 Wm^{-2} are also made in the Bay of Bengal. The remaining areas have adjustments associated with aerosols that have probably been transported by westerly winds. In the Pacific region adjacent to the coast of China the adjustment has a maximum of 40-50 Wm^{-2} which diminishes rapidly toward the east. However a plume representing adjustments of up to 10 Wm^{-2} is evident stretching northeast to the central North Pacific. A smaller and weaker area of adjustment is also evident off the east coast of North America and in the Gulf of Mexico.

Considering the global ocean, the mean adjustment to the shortwave by the Tragou method is 2.0 Wm^{-2}. If this is taken to be an upper limit, it would appear that the aerosol effect accounts for only about 7% of the existing bias in the SOC climatology of 30 Wm^{-2} discussed by Josey et al. (1999). Thus, although potentially important at a regional level, particularly in the Tropics, neglect of aerosols does not appear to be a major factor in explaining the global heat budget imbalance.

4.3 Buoy - SOC Difference Versus SAOT

Having quantified the likely impact of the aerosol effect on the original SOC shortwave estimates we now attempt to determine whether these estimates are supported by independent datasets. Unfortunately, there are few high quality shortwave measurements available and this has limited this part of our study. We begin by carrying out a comparison of original shortwave flux

at the sites of the various WHOI buoy deployments with the corresponding values measured by the buoys (for more details of this technique see Josey et al., 1999). A scatter plot of the difference between the original SOC shortwave and direct measurements from buoys against the SAOT is shown in Fig. 5.

Out of the ten buoys shown, only 3 experienced the conditions of moderate to high aerosol loading (SAOT >0.1) necessary to determine whether there is a direct relationship between shortwave bias and SAOT. For these 3 buoys (SE Subduction, FASINEX and Arabian Sea), the difference of SOC from the buoy increases from about –15 to 15 Wm^{-2} as the SAOT increases from about 0.15 to 0.23. Thus, the sense of the trend is consistent with the idea that higher aerosol loading will lead to an increase in the SOC shortwave flux relative to the buoy measurements. However, it should be noted that the absolute value of the TOGA buoy flux is still 15 Wm^{-2} less than the buoy value despite being in a region of moderate aerosol loading (SAOT=0.15). It is not possible to say at this stage whether, this reflects another source of bias or a problem with the aerosol loading hypothesis.

The remaining 7 buoys all experienced aerosol loading similar to that at the stations originally used by Reed (1977, SAOT about 0.05) and thus cannot be used to test the hypothesis, The fact that they show a large scatter up to 20 Wm^{-2} about the zero line demonstrates that there are considerable sources of difference between the buoy and SOC values even in the absence of the aerosol effect. The scatter may reflect the sampling error that is expected when the SOC fluxes which are based on a limited number of ship observations are compared with the high frequency, complete time series buoy values. We note that it would be instructive to correlate the difference between buoy estimates and the adjusted shortwave with the aerosol loading. However, the available satellite aerosol data does not cover the time periods of the buoy deployments for the majority of the moorings considered, hence such a comparison is not possible at present.

It is possible that the weak correlation noted above between the error in the Reed formula and that from aerosol loading also reflects problems in accurately accounting for the attenuation of solar radiation by clouds. Medovaya et al. (2002) also found a weak correlation between modeled shortwave minus that observed at various buoys and the aerosol loading when they considered clear skies conditions only. They suggested that the poor correlation may have been because the limited number of observations from the AVHRR product prevented an adequate representation of the relationship. One problem is that the aerosol type affects the amount of attenuation. The aerosol type, which is not characterised by the AVHRR product, varies from region to region and even within regions such as the Subduction zone (Waliser et al., 1999). In addition to this, the errors associated with buoy shortwave measurements are not yet completely understood and quantifiable. Problems associated with shortwave sensor tilt or salt build up on the sensors were dealt with only qualitatively by Medovaya et al. (2002) and they note that there may be other problems associated with the ‘stressful and remote operating environment’ of the buoys.

4.4 Comparison with Satellite Based Measurements of Shortwave Flux

In addition to the buoy comparisons, we have also considered independent satellite based estimates of the shortwave flux contained in the LPSA and FD datasets described in Section 2. A comparison between the shortwave flux fields of SOC and LPSA for 1986 and 1992 is shown in

Figs. 6 and 7. It is worth noting that the LPSA fields have some discontinuities, (particularly in the Indian Ocean) associated with the geographical range of the different satellites used to derive the global fields. Because the discontinuities are unphysical, it is appropriate to be cautious about the level of confidence placed in the LPSA fields. However, we will comment on the Atlantic Ocean as it is largely free of these discontinuities and shows some interesting differences with the SOC shortwave. SOC estimates more shortwave than LPSA in the northwestern region of the North Atlantic and in the southwestern region of the South Atlantic. In contrast, SOC has less shortwave than LPSA in the southeastern region of the North Atlantic and in the northeastern region of the South Atlantic. These differences are locally of the order ±40 Wm^{-2} and are not related to aerosol loading as there is very little spatial variability of aerosol in LPSA. A comparison of global fields of SOC cloud cover and the ISCCP cloud cover used in LPSA is shown in Fig. 8. These fields suggest that a large proportion of the difference can be explained by the different estimates of cloud cover in the two data sets as the SOC cloud cover is higher/lower in the regions where the shortwave is less/greater than LPSA.

A comparison between the shortwave flux fields of SOC and FD shortwave for 1986 and 1992 are shown in Figs. 9 and 10. The areas where the SOC estimate is more than 15 Wm^{-2} greater than the satellite product tend to coincide with areas where the aerosol loading is high. Thus, this comparison provides some support for the idea that neglect of aerosols has led to the SOC shortwave flux being biased high in regions of strong loading. Dr. Zhang of Columbia University has provided examples of the total aerosol optical thickness used in the calculation of the FD shortwave flux for JAJO of 1991 (Fig. 11). It is evident that the same regions of high aerosol loading from the AVHRR data (Fig. 2) are described in the input for the FD algorithm (Fig. 11). Not all of the differences between SOC and FD can be attributed to the presence of aerosols in the FD algorithm. For example, there are some areas in the southern ocean where the relatively low FD flux appears unrelated to the aerosols. In addition in Fig. 9c there is also a thin band in the Tropical Pacific that is probably associated with a different location of the ITCZ rather than the presence of aerosols.

It is also interesting to note that the global mean shortwave flux from LPSA and FD indicated on the figures is typically 2 - 4 Wm^{-2} greater than that estimated from SOC. Thus the satellite data does not suggest that the 30 Wm^{-2} bias in the SOC heat budget is due to an overestimate of the shortwave in the global mean.

5. SUMMARY

An attempt to quantify the effect that neglect of aerosol loading has had on estimates of the shortwave flux in the SOC climatology has been described. Adjustments for this aerosol effect were made using the method of Tragou et al. (1999) with AVHRR estimates of satellite aerosol optical thickness (SAOT). The spatial coverage and resolution of the AVHRR product makes it compatible with the SOC data set. In addition, the spatial and temporal patterns depicted by the SAOT are in agreement with existing knowledge of aerosol distribution. Although there are a couple of features in the SAOT fields that are not in known areas of high aerosol loading, these have a relatively minor impact on the shortwave field. The adjusted fields suggest that the aerosol effect accounts for less than 7% or 2 Wm^{-2} of the 30 Wm^{-2} bias in the SOC heat flux

climatology. However, in areas of high aerosol loading, such as the Red Sea, the Gulf of Arabia, the Arabian Sea, the Bay of Bengal, the North-West Pacific and the Tropical Atlantic, the aerosol adjustment was estimated to be up to 40 Wm^{-2} in the annual mean.

We have attempted to validate the existence of the aerosol effect with independent estimates of shortwave radiation from buoys and satellites. The results of these comparisons are severely limited by the availability of high quality buoy measurements but provide some support for the aerosol effect. For a subset of 3 buoys at sites with mid-high aerosol loading there was some evidence for an overestimate of the original SOC shortwave flux (relative to the research buoy) being associated with anomalously high aerosol loading. The other buoys considered are in a region of low aerosol loading and showed a large scatter indicating that other processes are likely to be important sources of error. Comparison of the SOC shortwave with the satellite derived FD flux product indicated that SOC overestimated shortwave relative to FD in regions of strong aerosol loading.

In conclusion, our calculations suggest that the aerosol effect may account for about 2 Wm^{-2} of the 30 Wm^{-2} global mean net heat flux bias in the SOC climatology. At a regional level biases in the shortwave flux may be much larger with values up to 40 Wm^{-2} in the Tropical Atlantic. However, further comparisons against a greater sample of high quality shortwave measurements from planned surface flux reference sites are required to confirm our results.

ACKNOWLEDGEMENTS

The work described in this report has been funded as part of the NERC COAPEC thematic programme under the project: Balancing the Atlantic Heat and Freshwater Budgets, Ref. NER/T/S/2000/00314.

REFERENCES

Barkstrom, B. R., E. F. Harrison, G. L. Smith, R. N Green, J. F. Kibler, R. D. Cess, and the ERBE Science Team, 1989: Earth Radiation Budget Experiment archival and April 1985 results. *Bull. Amer. Meteor. Soc.,* **70**, 1254-1262.

Chin, M., D. J. Jacob, G. M. Gardner, M. S. Foreman-Fowler, P. A. Spiro and D. L. Savoie, 1996: A global three-dimensional model of tropospheric sulfate. *J. Geophys. Res.*, **101**, 18667-18690.

Gilman, C., and C. Garrett, 1994: Heat flux parameterizations for the Mediterranean Sea: The role of atmospheric aerosols and constraints from the water budget. *J. Geophys. Res.*, **99**(C3), 5119-5134.

Grist, J. P. and S. A. Josey, 2003: Inverse analysis adjustment of the SOC air-sea flux climatology using ocean heat transport constraints. *J. Climate,* **16,** 3274-3295.

Grist, J. P. and S. A. Josey, 2004: Closing the heat budget of the SOC climatology through spatially dependent inverse analysis parameter adjustment, Southampton Oceanography Centre Research and Consultancy Report, in preparation.

Gupta, S. K., D. P. Kratz, P. W. Stackhouse, Jr. and A. C. Wilber, 2001: The Langley Parameterized Shortwave Algorithm (LPSA) for Surface Radiation Budget Studies. Version 1.0, NASA /TP- 2001-211272, Langley Research Center, Hampton, Virginia, 23681-2199.

Husar, R. B., J. M. Prospero and L. L. Stowe, 1997: Characterization of tropospheric aerosols over the oceans with the NOAA advanced very high resolution radiometer optical thickness operational product. *J. Geophys. Res.*, **102**(D14), 16889-16909.

Josey, S. A., E. C. Kent and P. K. Taylor, 1998: The Southampton Oceanography Centre (SOC) Ocean - Atmosphere Heat, Momentum and Freshwater Flux Atlas. *Southampton Oceanography Centre Report No. 6, Southampton, UK*, 30 pp. & figs.

Josey, S. A., E. C. Kent and P. K. Taylor, 1999: New insights into the ocean heat budget closure problem from analysis of the SOC air-sea flux climatology. *J. Climate*, **12**(9), 2856-2880.

Josey, S. A., R. W. Pascal, P. K. Taylor and M. J. Yelland, 2003: A new formula for determining the atmospheric longwave flux at the ocean surface at mid-high latitudes. *J. Geophys. Res.,* **108**(C4), doi:10.1029/2002JC001418.

Kent, E. C., R. J. Tiddy and P. K. Taylor, 1993: Correction of marine daytime air temperature observations for radiation effects. *J. Atmos. & Oceanic Tech.*, **10**(6), 900-906.

Lacis, A. A. and M. I. Mishchenko, 1995: Climate forcing, climate sensitivity, and climate response: A radiative modeling perspective on atmospheric aerosols. *Aerosol Forcing of Climate*, R. J. Charlson and J. Heintzenberg, Ed., John Wiley, 11-42.

Medovaya, M., D. E. Waliser, R. A. Weller and M. J. McPhaden, 2002: Assessing ocean buoy shortwave observations using clear-sky model calculations. *J. Geophys. Res.*, **107**(C2): art. no. 3014 FEB 15.

Moyer, K. A. and R. A. Weller, 1997: Observations of surface forcing from the Subduction Experiment : a comparison with global model products and climatological data sets. J. Clim., **10**(11), 2725 - 2742.

Payne, R. E., 1972: Albedo of the sea surface. *J. Atmos. Sci.*, **29**, 959-970.

Reed, R. K., 1977: On estimating insolation over the ocean. *J. Phys. Oceanogr.*, **7**, 482-485.

Rosati, A. and K. Miyakoda, 1988: A general circulation model for upper ocean simulation. *J. Phys. Oceanogr.,* **18,** 1601-1626.

Rossow, W. B. and R. A. Schiffer, 1991: ISCCP Cloud Data Products. *Bull. Amer. Meteor. Soc.,* **72**, 2-20.

Seckel, G. R. and F. H. Beaudry, 1973: The radiation from sun and sky over the Pacific Ocean (Abstract). *Trans. Amer. Geophys. Union,* **54,** 1114.

Stowe, L. L., A. M. Ignatov and R. R. Singh, 1997: Development, validation, and potential enhancements to the second-generation operational aerosol product at the National Environmental Satellite, Data, and Information Service of the National Oceanic and Atmospheric Administration. *J. Geophys. Res.*, **102**(D14), 16923-16934.

Tragou, E., C. Garrett and R. Outerbridge, 1999: The heat and freshwater budgets of the Red Sea. *J. Phys. Oceanogr.*, **29**(10), 2504-2522.

Tragou, E. and A. Lascaratos, 2003: The effect of aerosols on the Mediterranean solar radiation budget. *J. Geophys. Res.*, (C2) art no. 3025 Feb. 11.

Waliser, D. E, R. A. Weller, and R. D. Cess, 1999: Comparisons between buoy-observed, satellite-derived and modeled surface shortwave flux over the subtropical North Atlantic during the Subduction Experiment. *J. Geophys. Res.,* **104**(D24), 31301-31320.

Wang, J., W. B. Russo and Y. Zhang, 2000: Cloud vertical structure and its variations from a 20-year global rawinsonde dataset. *J. Climate*, **13,** 3041-3056.

WMO, 1993: International list of selected, supplementary and auxiliary ships. WMO Rep. 47, 264 pp.

Woodruff, S. D., S. J. Lubker, K. Wolter, S. J. Worley and J. D. Elms, 1993: Comprehensive Ocean-Atmosphere Data Set (COADS) release 1a: 1980-92. *Earth System Monitor*, **4**(1), 4-8.

Zhang, Y-C., W. B. Rossow, A. A. Lacis, V. Oinas and M. I. Mishchenko, 2003: Calculation of radiative flux profiles from the surface to top-of-atmosphere based on ISCCP and other global datasets: Refinements of the radiative transfer model and the input data. *J. Geophys. Res.,* in preparation.

TABLES

Name of Research Buoy	Date of deployment	Location	Difference in Shortwave Flux (SOC– buoy) Wm^{-2}	SAOT
Subduction (northeast)	June 1991 - June 1993	33.0° N, 22.0° W	-13	0.052
Subduction (southeast)	Mar. 1992 - June 1993	18.0° N, 22.0° W	13	0.220
Subduction (southwest)	June 1991 - June 1993	18.0° N, 34.0° W	-16	0.152
Subduction (northwest)	Mar. 1991 - Mar. 1992	33.0° N, 34.0° W	-14	0.047
Subduction (central)	June 1991 - June 1993	25.5° N, 29.0° W	-15	0.056
FASINEX	Feb. 1986 - May 1986	27.0° N, 70.0° W	-2	0.064
TOGA-COARE	Nov. 1992 - Feb. 1993	1.8° S, 156.0° E	23	0.049
Arabian Sea	Oct. 1994 - Oct. 1995	15.5° N, 61.5° E	-3	0.178
Equatorial North Pacific	May 1997 - Dec. 1997	10° N, 125.5° W	7	0.054
Equatorial South Pacific	May 1997 - Dec. 1997	2.5° S, 124.5° W	-2	0.048

Table 1. Details of the Various WHOI Buoy Deployments Used in this Study.

FIGURE CAPTIONS

Fig. 1) Original SOC fields (1980-93) for mean shortwave radiation (Wm^{-2}) for a) January, b) April, c) July and d) October.

Fig. 2) AVHRR data of satellite derived aerosol optical thickness (SAOT) (dimension-less) for a) January, b) April, c) July and d) October. Mean monthly values for the period July 1989 – June 1991.

Fig. 3) Global fields of the transmission coefficient anomaly (dimension-less) for a) January, b) April, c) July and d) October. Mean monthly values for the period July 1989 – June 1991.

Fig. 4) Annual mean shortwave surface radiation from the a) original SOC field, b) adjusted field and c) adjusted field minus original field. Units are Wm^{-2}.

Fig. 5) Scatter plot of SOC shortwave minus buoy shortwave versus SAOT at 10 buoys for the period of each buoy deployment (see Table 1). Northeast Subduction buoy (red x), southeast Subduction buoy (green x), southwest Subduction buoy (blue x), northwest Subduction buoy (cyan x), central Subduction buoy (magenta x), FASINEX (black triangle), TOGA-COARE (black cross), Arabian Sea (black star), equatorial North Pacific (black circle), equatorial South Pacific (black square).

Fig. 6) Shortwave surface radiation 1986 for; a) original SOC field, b) LPSA, and c) SOC – LPSA. Units are Wm^{-2}. The global mean difference between SOC and LPSA is –4 Wm^{-2}.

Fig. 7) Shortwave surface radiation 1992 for; a) original SOC field, b) LPSA, and c) SOC – LPSA. Units are Wm^{-2}. The global mean difference between SOC and LPSA is –5 Wm^{-2}.

Fig. 8) Fractional cloud cover over the global ocean 1986 from a) SOC, b) LPSA (ISCCP) and c) SOC – LPSA.

Fig. 9) Shortwave surface radiation 1986 for; a) original SOC field, b) FD data set and c) SOC – FD. Units are Wm^{-2}. The global mean difference between SOC and FD is –8 Wm^{-2}.

Fig. 10) Shortwave surface radiation 1992 for; a) original SOC field, b) FD data set and c) SOC – FD. Units are Wm^{-2}. The global mean difference between SOC and FD is –4 Wm^{-2}.

Fig. 11) Total Aerosol Optical Thickness (dimension-less) from the GISS GCM. Fields are the monthly means for a) January 1991, b) April 1991, c) July 1991 and d) October 1991.

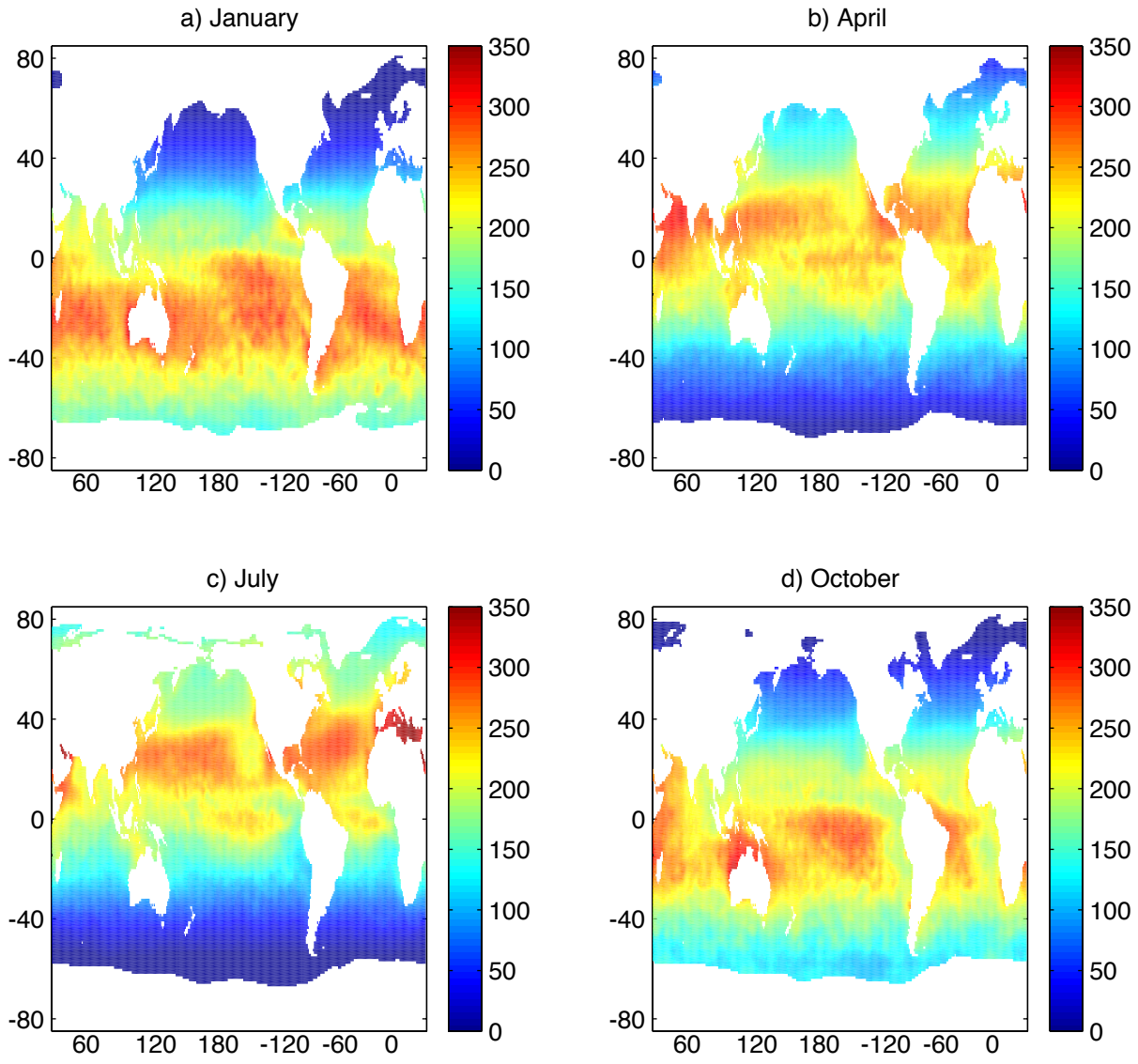

Fig. 1) Original SOC fields (1980-93) for mean shortwave radiation (Wm^{-2}) for a) January, b) April, c) July and d) October.

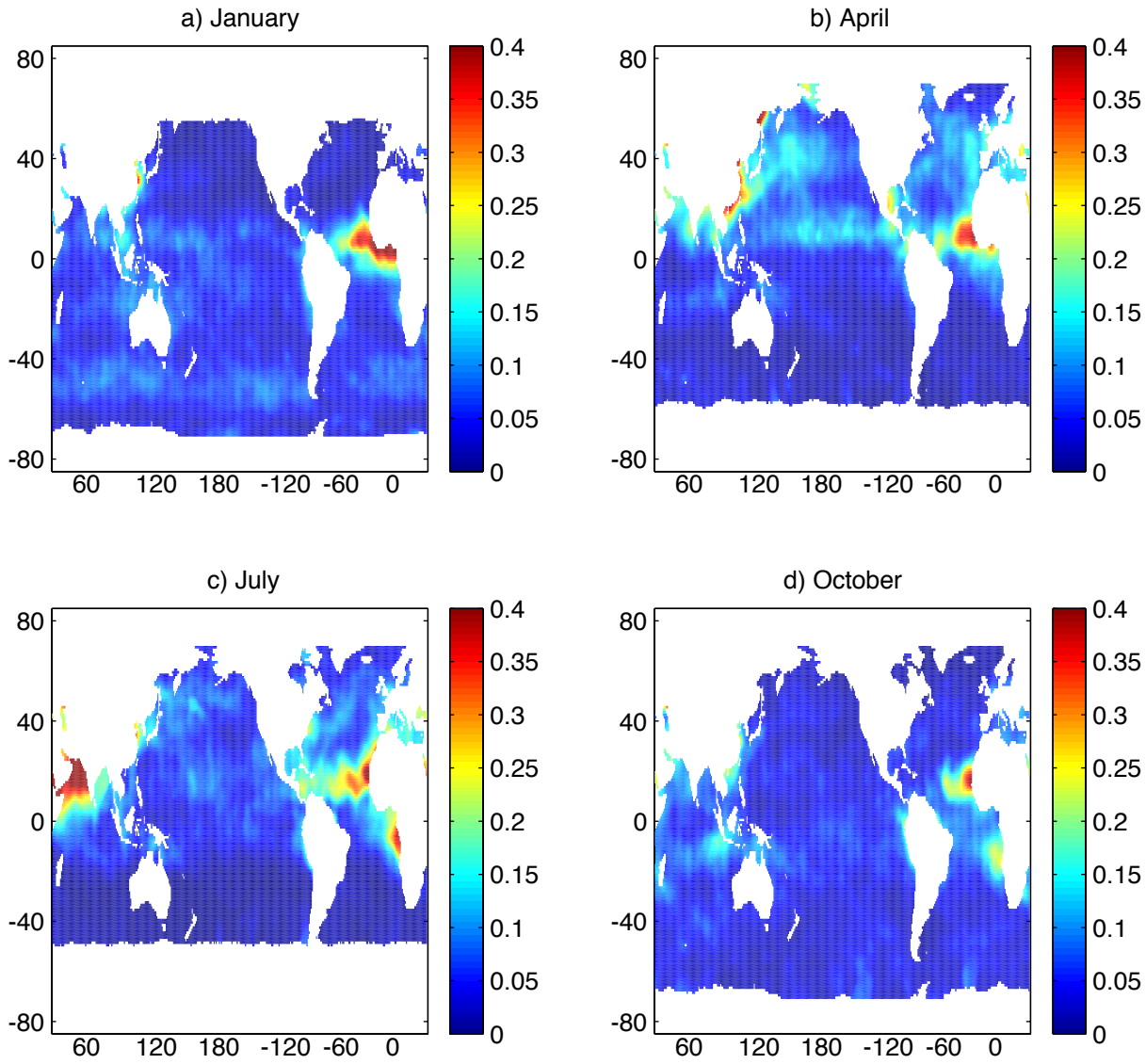

Fig. 2) AVHRR data of satellite derived aerosol optical thickness (SAOT) (dimension-less) for a) January, b) April, c) July and d) October. Mean monthly values for the period July 1989 b June 1991.

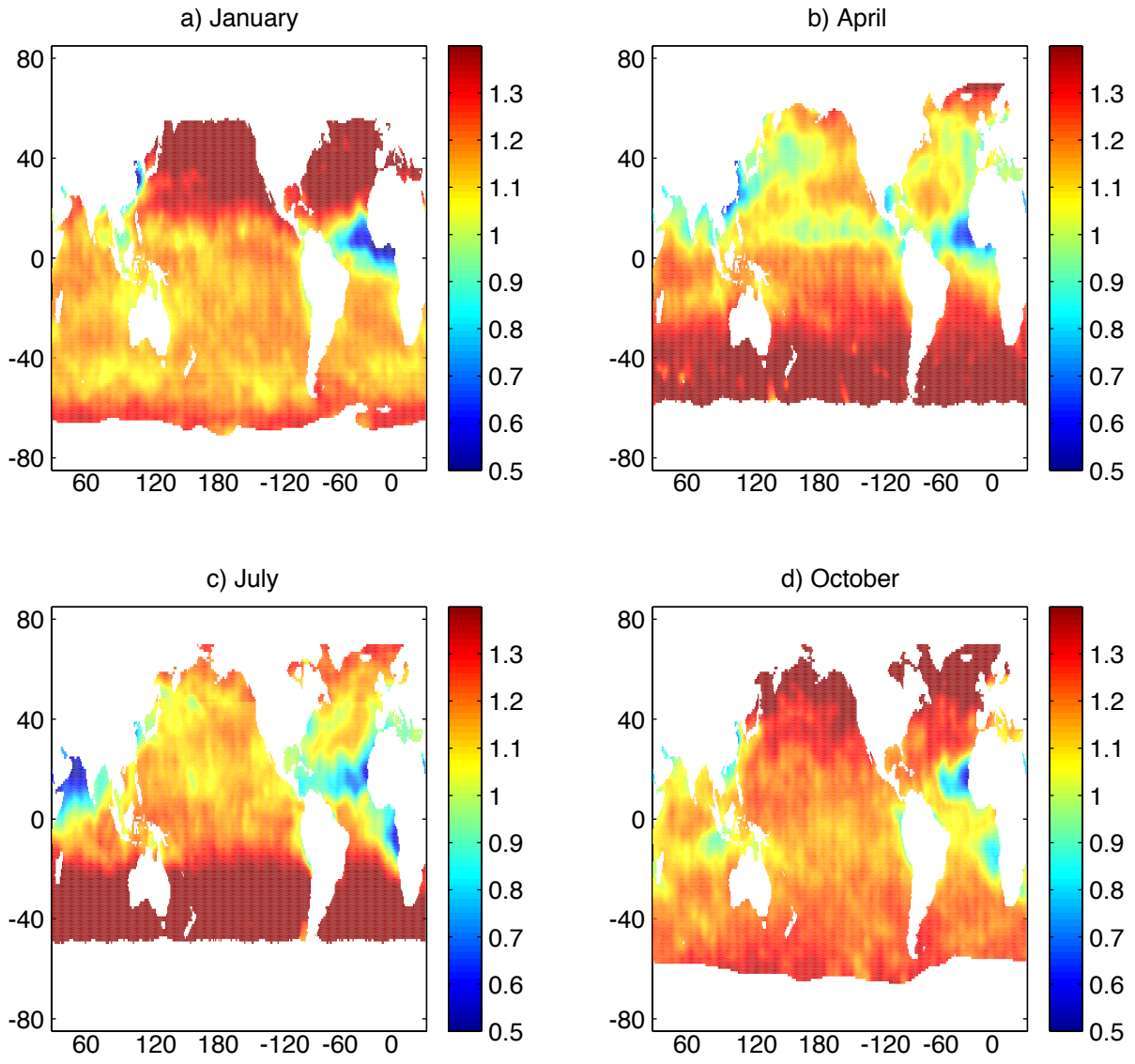

Fig. 3) Global fields of the transmission coefficient anomaly (dimension-less) for a) January, b) April, c) July and d) October. Mean monthly values for the period July 1989 b June 1991.

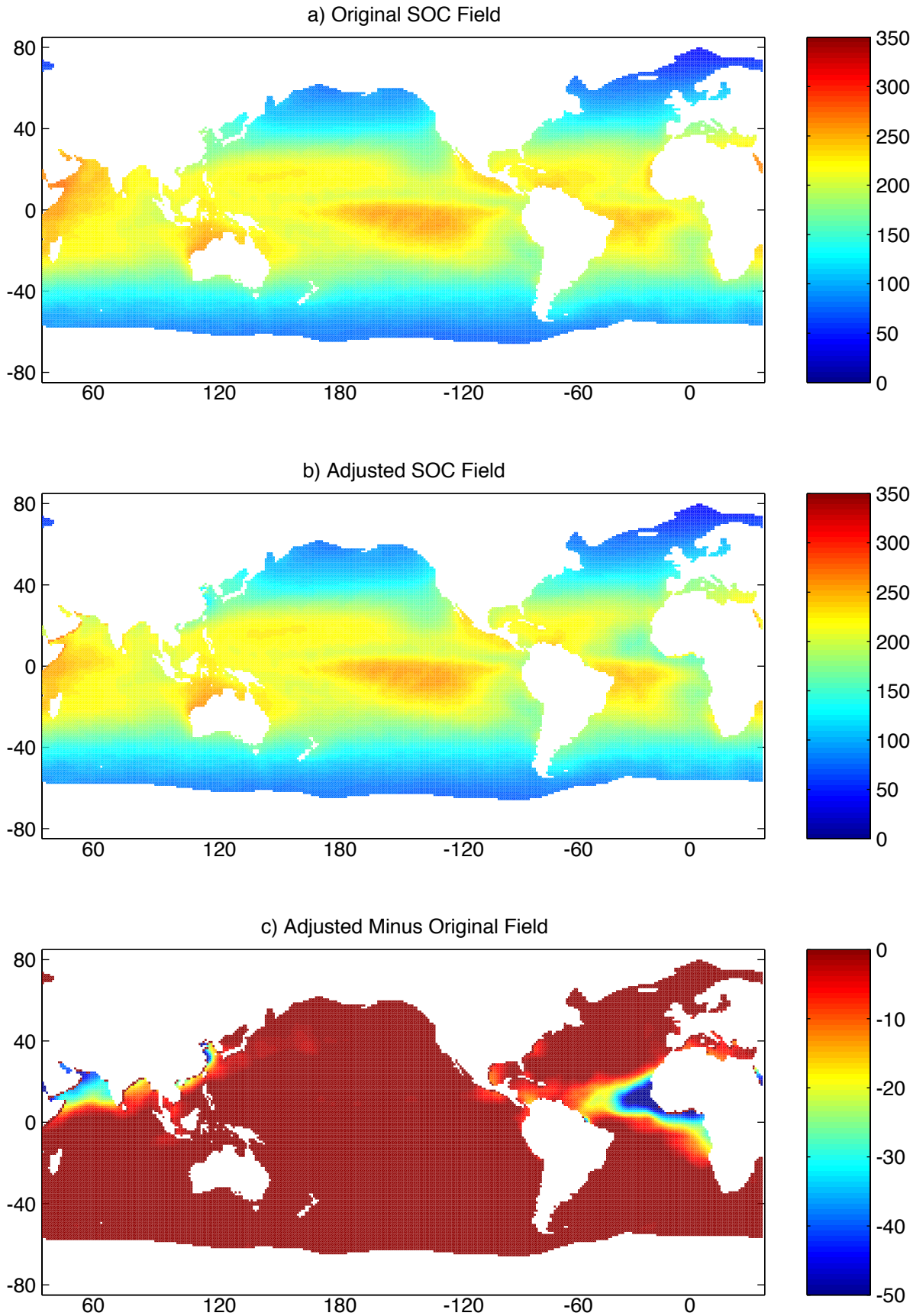

Fig. 4) Annual mean shortwave surface radiation from the a) original SOC field, b) adjusted field and c) adjusted field minus original field. Units are Wm^{-2}.

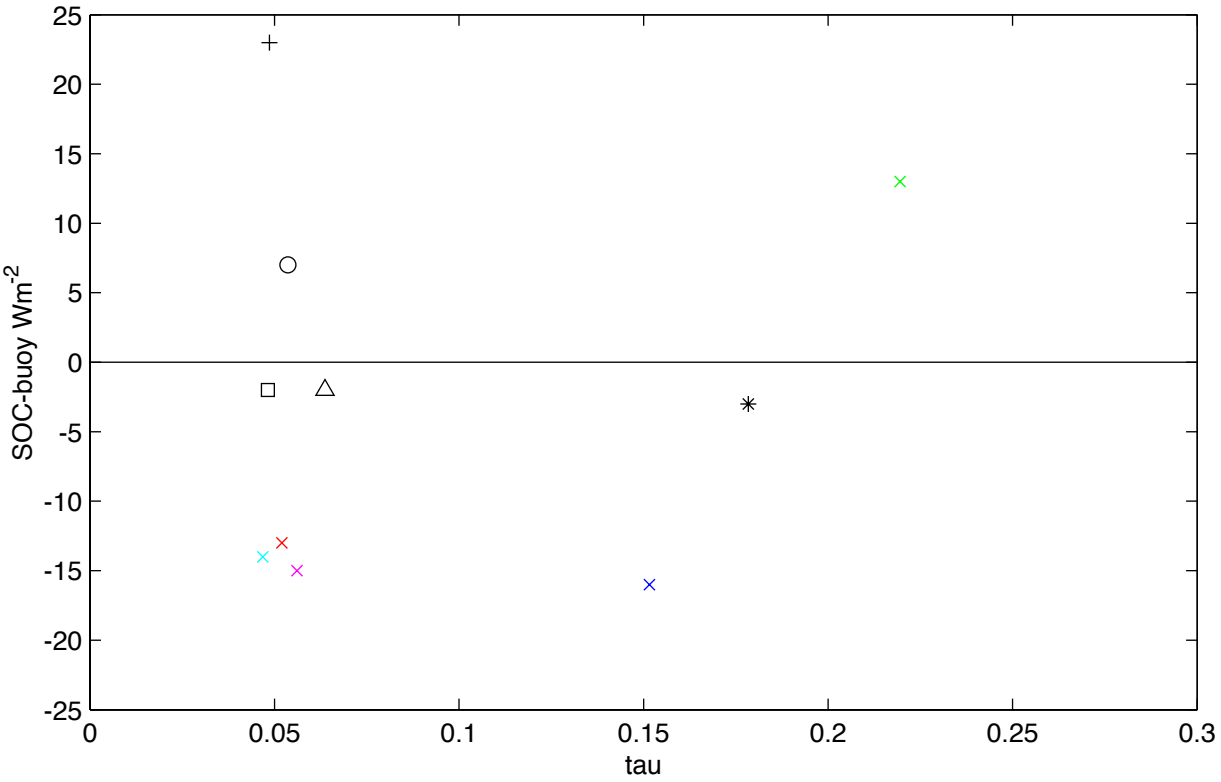

Fig. 5) Scatter plot of SOC shortwave minus buoy shortwave versus SAOT at 10 buoys for the period of each buoy deployment (see Table 1). Northeast Subduction buoy (red x), southeast Subduction buoy (green x), southwest Subduction buoy (blue x), northwest Subduction buoy (cyan x), central Subduction buoy (magenta x), FASINEX (black triangle), TOGA-COARE (black cross), Arabian Sea (black star), equatorial North Pacific (black circle), equatorial South Pacific (black square).

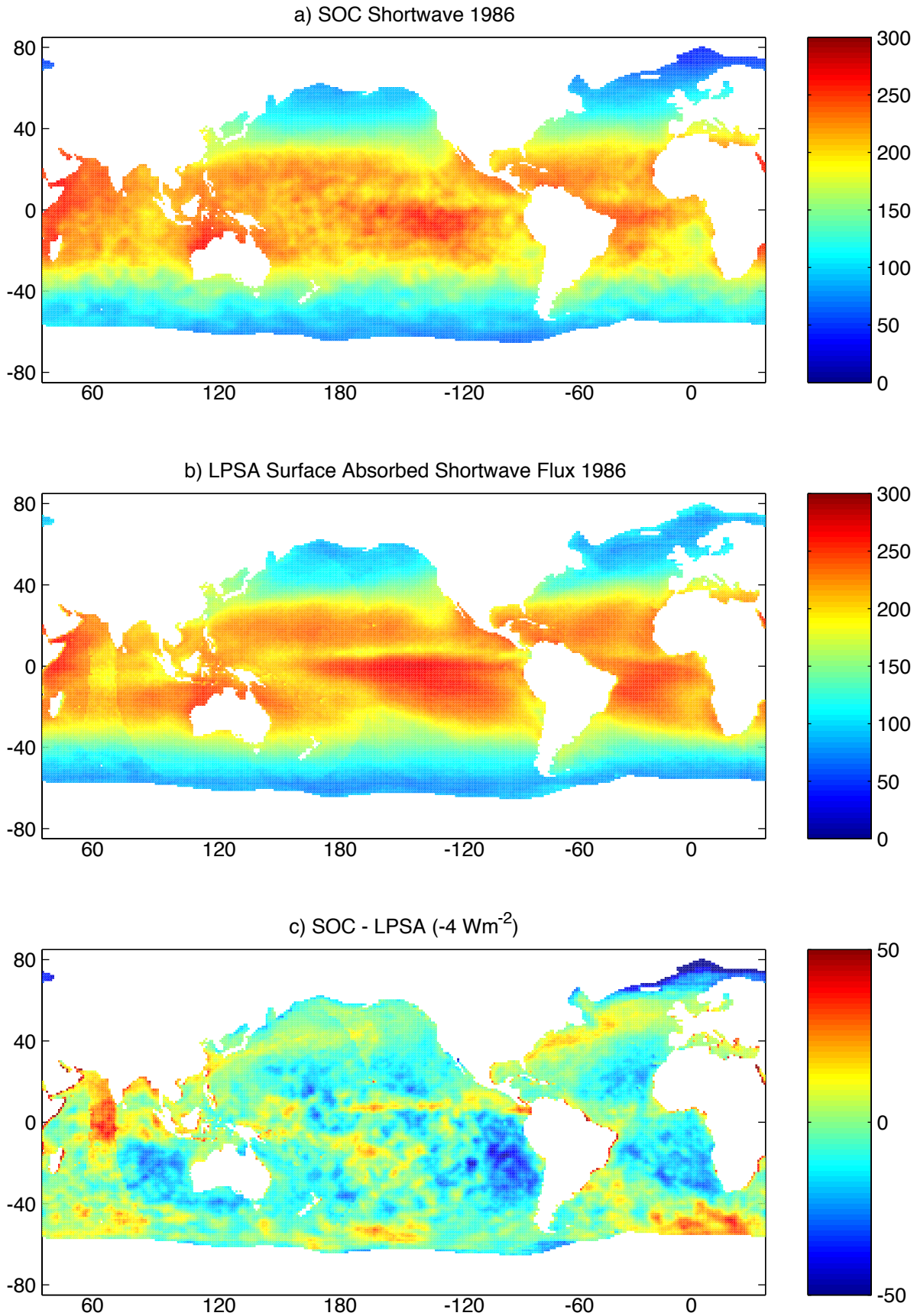

Fig. 6) Shortwave surface radiation 1986 for; a) original SOC field, b) LPSA, and c) SOC b LPSA. Units are Wm^{-2}. The global mean difference between SOC and LPSA is -4 Wm^{-2}.

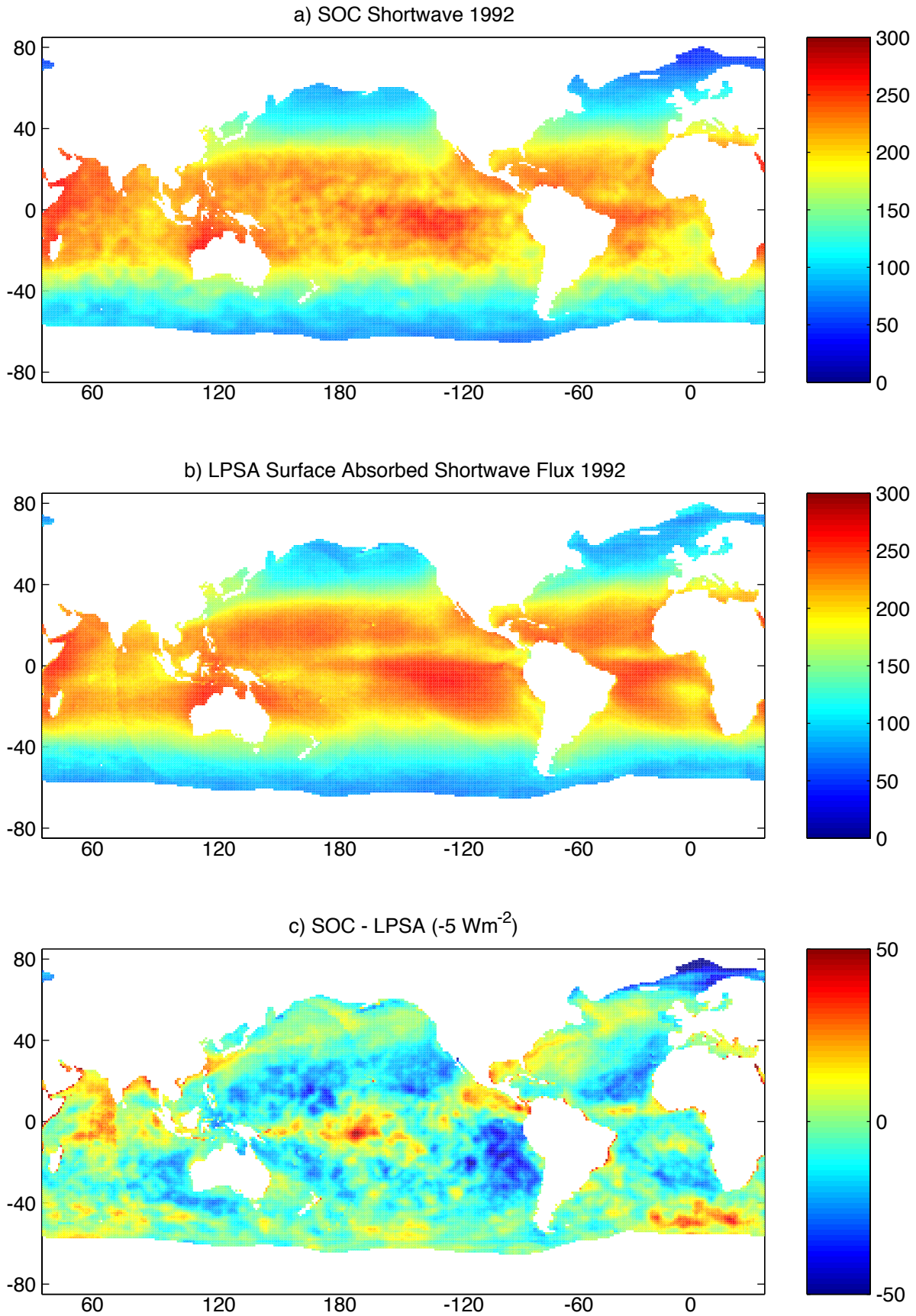

Fig. 7) Shortwave surface radiation 1992 for; a) original SOC field, b) LPSA, and c) SOC b LPSA. Units are Wm^{-2}. The global mean difference between SOC and LPSA is -5 Wm^{-2}.

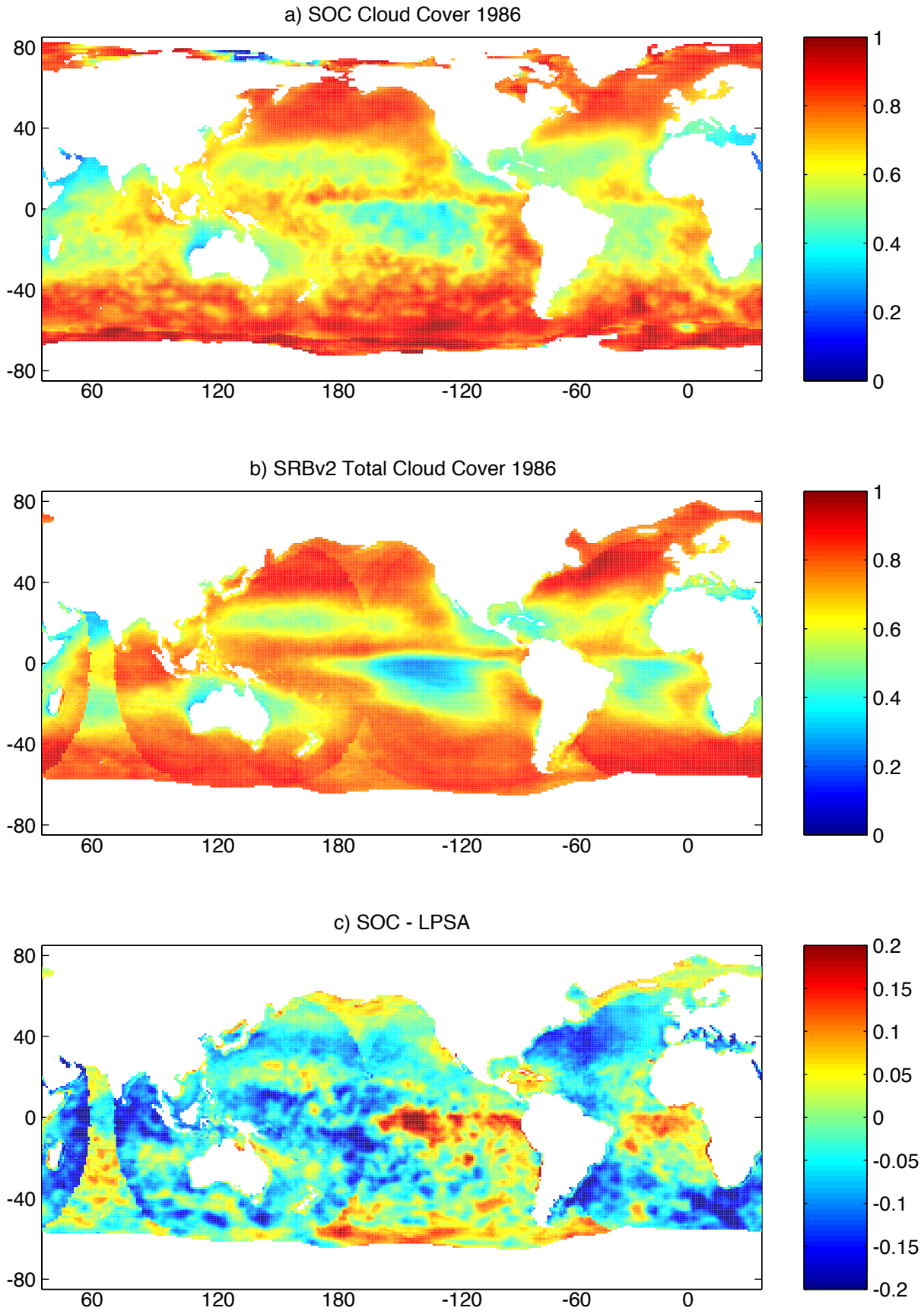

Fig. 8) Fractional cloud cover over the global ocean 1986 from a) SOC, b) LPSA (ISCCP) and c) SOC - LPSA.

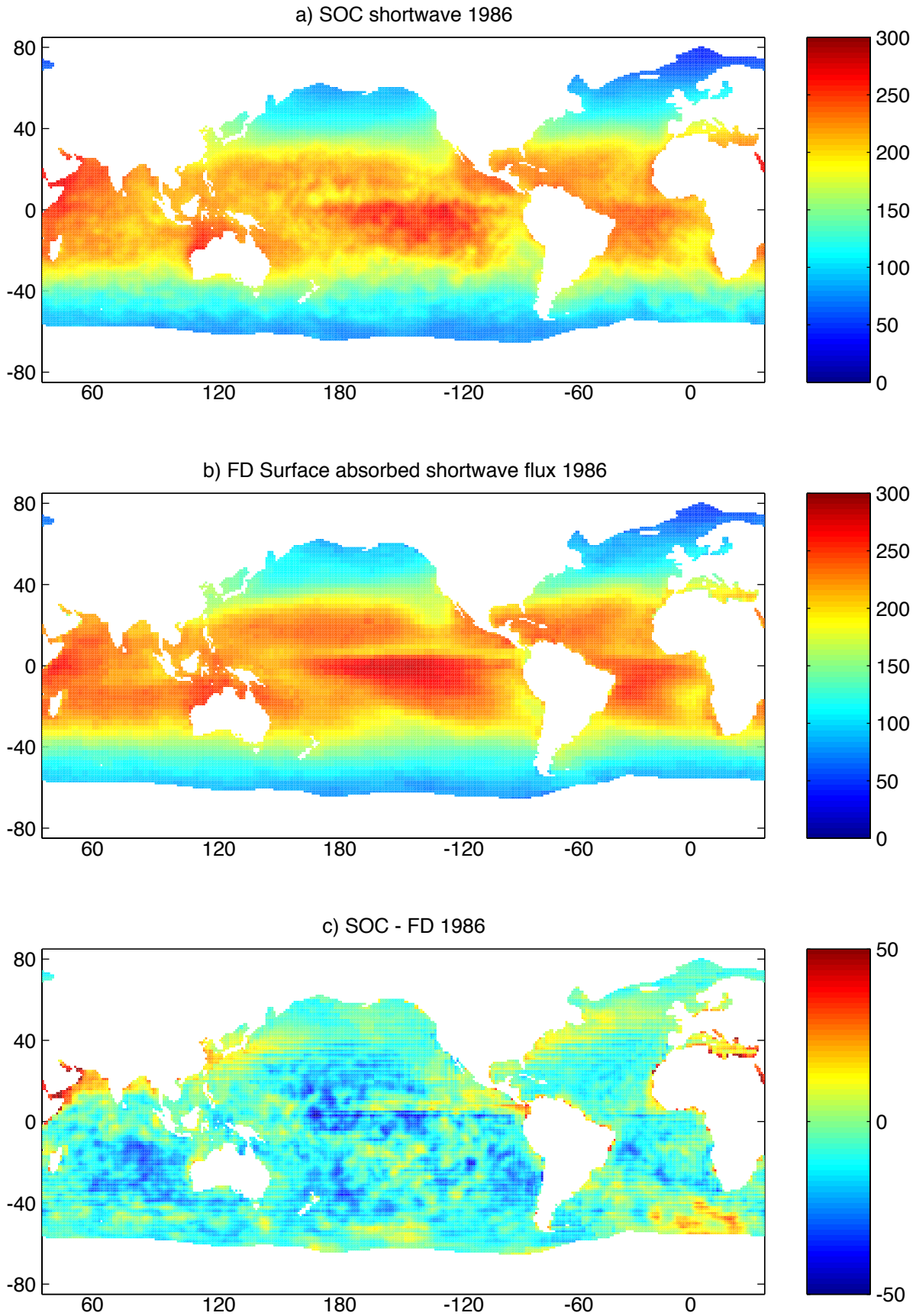

Fig. 9) Shortwave surface radiation 1986 for; a) original SOC field, b) FD data set and c) SOC - FD. Units are Wm^{-2}. The global mean difference between SOC and FD is -8 Wm^{-2}.

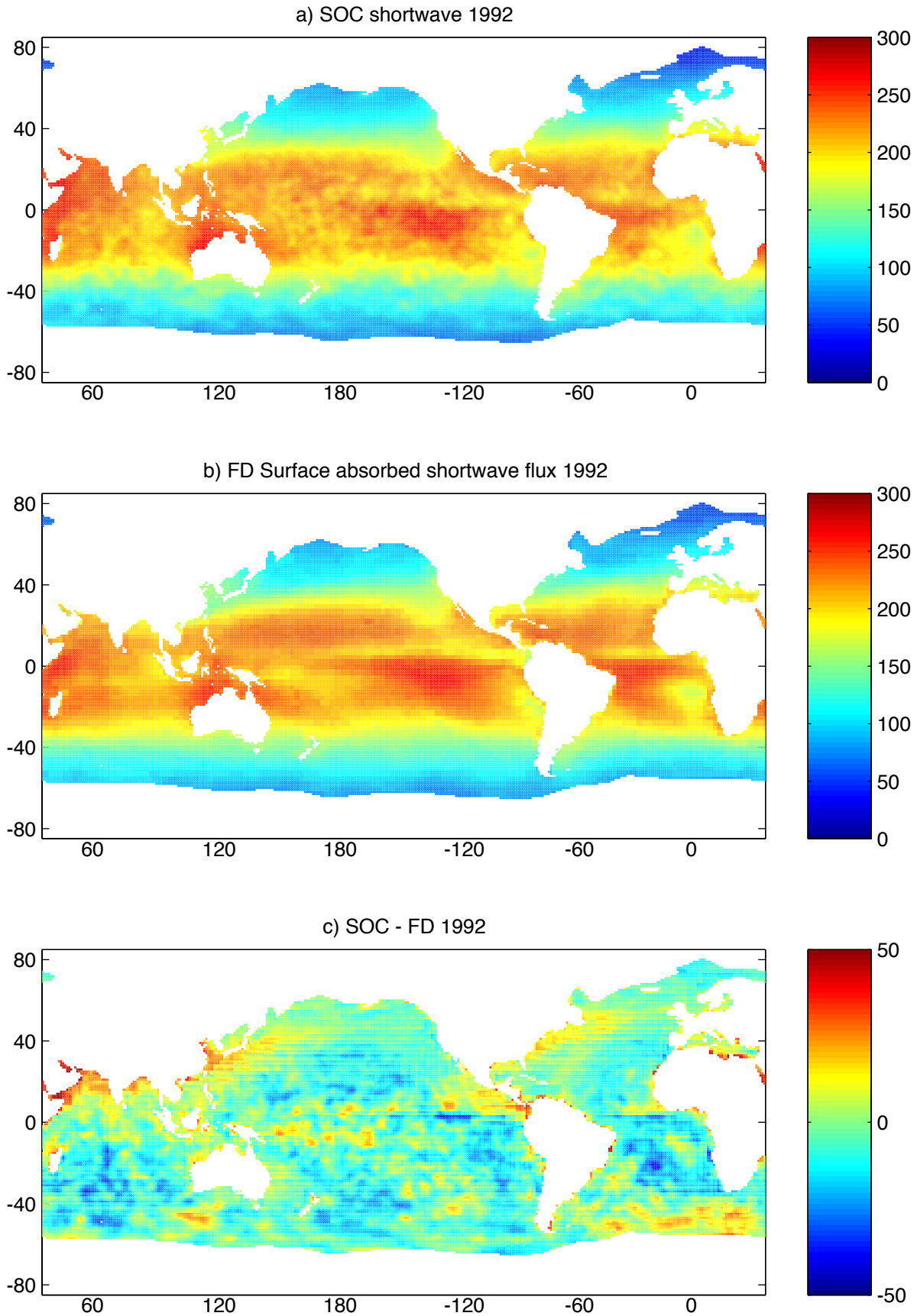

Fig. 10) Shortwave surface radiation 1992 for; a) original SOC field, b) FD data set and c) SOC - FD. Units are Wm^{-2}. The global mean difference between SOC and FD is -4 Wm^{-2}.

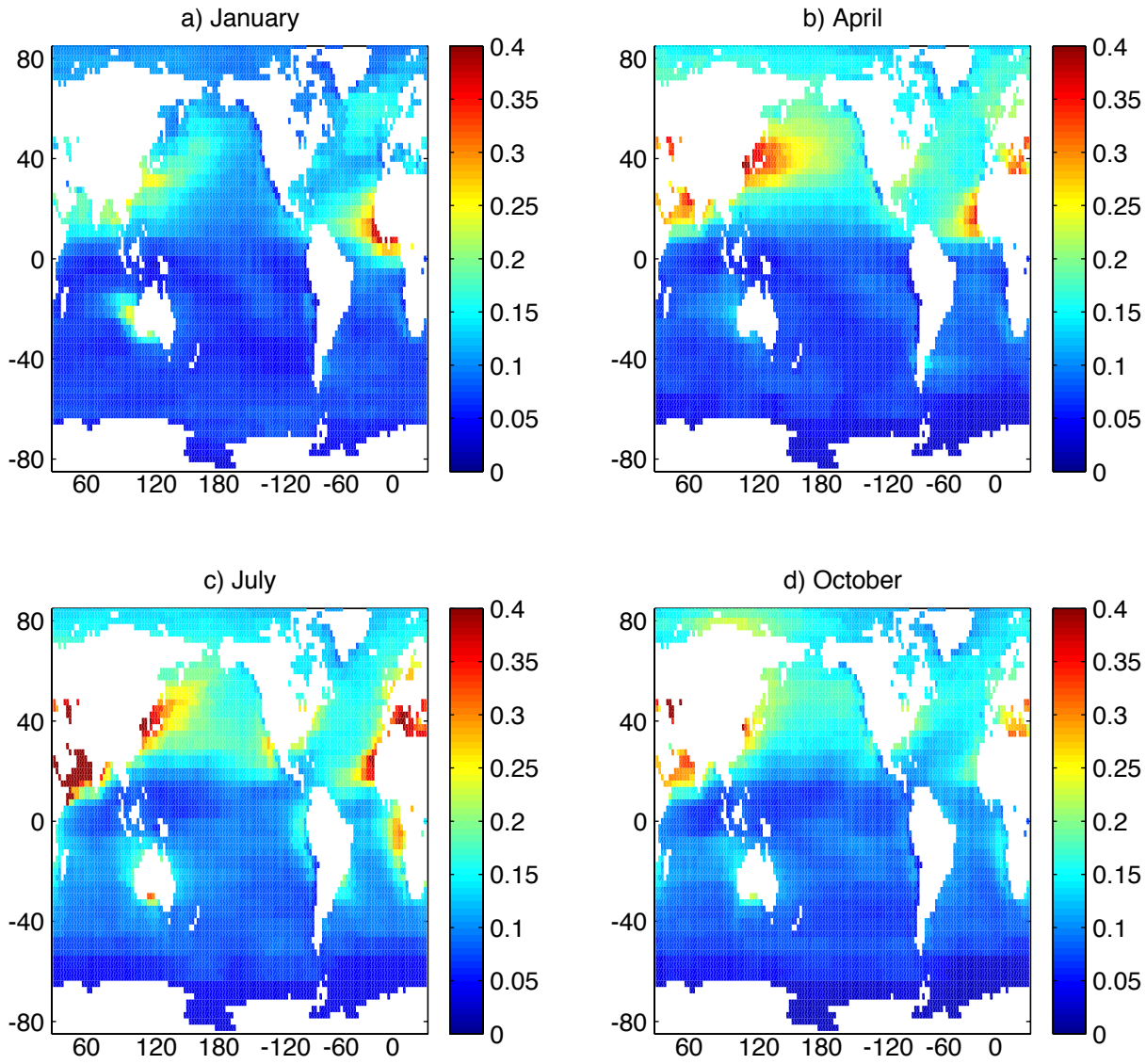

Fig. 11) Total Aerosol Optical Thickness (dimension-less) from the GISS GCM. Fields are the monthly means for a) January 1991, b) April 1991, c) July 1991 and d) October 1991.